

# The Propagation Time of a Radio Pulse\*

J. RALPH JOHLER†, SENIOR MEMBER, IEEE

**Summary**—The propagation of the ground-wave pulse between points on the ground is of considerable practical importance, particularly in the application of the Loran-C navigation system to the absolute time synchronization of geographically separated clocks. Thus, the envelope of the pulse is frequently used to remove ambiguities which would otherwise result from the pulse synchronization at the characteristic or carrier frequency of the pulse.

The propagation of the ground wave over finitely conducting ground modifies the propagation time of the tagged point-in-time on the envelope by amounts which may be sufficiently large as to cause cycle ambiguity  $\pm\pi$  radians at the carrier or characteristic frequency of the pulse. It is therefore the purpose of this paper to investigate the magnitude of this error by ascertaining the true signal velocity as determined by tagging a point-in-time on the leading edge of a groundwave pulse and calculating the time corrections for various ground conductivities and distances. These calculations can then be applied to resolve the  $\pm\pi$  radians ambiguity of the precision phase velocity instrumentation for Loran-C especially when the system is used for absolute-time synchronization.

## INTRODUCTION

THE APPLICATION of the Loran-C radio navigation system to the absolute synchronization of clocks separated geographically by thousands of miles to an accuracy better than one  $\mu\text{sec}$  requires a knowledge of the propagation time correction for the Loran-C radio navigation pulse at the point-in-time at which the synchronization is made.<sup>1-3</sup> Precise synchronization is ordinarily performed on the leading edge of the ground-wave pulse, since as a result of the ionospheric-wave delay,<sup>4</sup> the various ionospheric waves can be sorted from each other and from the ground wave with the system. This analysis will therefore treat the ground wave only, but the techniques are readily applied to ionospheric waves. The techniques based on the direct evaluation of the Fourier-transform integral have been discussed and summarized by Johler.<sup>4</sup> This paper applies these techniques to interpret the behavior of a defined point-in-time on the leading edge of a ground-wave radio navigation type pulse.

\* Received January 9, 1963; revised manuscript received May 8, 1963. This study was sponsored by the U. S. Dept. of the Navy, Office of Naval Research and U. S. Naval Observatory under Contract No. NAonr-11-62, Proposal P2-828 on NBS Project 85412 initiated under this contract.

† National Bureau of Standards, Boulder Laboratories, Boulder, Colo.

<sup>1</sup> R. H. Doherty, G. Hefley, and R. F. Linfield, "Timing potentials of Loran-C," *PROC. IRE*, vol. 49, pp. 1659-1673; November, 1961.

<sup>2</sup> G. Hefley, "Timing potentials of Loran-C, Signal J.," *Armed Forces Commun. and Electronics Assoc.*, vol. 15, pp. 45-47; February, 1961.

<sup>3</sup> W. P. Frantz, W. N. Dean, and R. C. Frank, "A precision multi-purpose radio navigation system," 1957 NATIONAL IRE CONVENTION RECORD, pt. 8, pp. 79-120; March 18-21, 1957.

<sup>4</sup> J. R. Johler, "Propagation of the low-frequency radio signal," *PROC. IRE*, vol. 50, pp. 404-427, April, 1962.

Two stages of detection are ordinarily employed in practice in the Loran-C system<sup>3</sup> for both radio navigation and precision clock synchronization. The first stage of detection identifies a point on the leading edge of the pulse by the amplitude envelope minus the time derivative of the amplitude envelope method and the corresponding cycle of the carrier. (Since this time, a more precise method for tagging a point-in-time on the pulse has been developed.<sup>5</sup>) This resolves the cycle ambiguity  $\pm 2\pi n$ , ( $n=0, 1, 2, 3 \dots$ ). The second stage is a vernier measurement which resolves a small fraction of the particular cycle originally identified. A recently developed method<sup>5</sup> for use with clock synchronization employs a measurement of a zero crossing of the cycle along with two crests (positive and negative) immediately preceding and following the zero crossing. The envelope and precision phase measurement are thus made in a single operation.

The radio navigation systems (Cytac, Loran-C) always measure the phase difference between signals received from a master and from a slave transmitter and, hence, measure the difference between these two phase difference measurements. The difference of the difference measurement thus became known as the discrepancy. Thus, even at great distances from the transmitter, the cycle ambiguity would tend to cancel in the difference of the difference measurement and show a small discrepancy, especially in the service area of the system where the distances to master and slave are approximately equal. However, to precisely synchronize a clock with such a system, it is necessary to know the precise point-in-time on the envelope, since in this case an error of  $\pm\pi$  or 10  $\mu\text{sec}$  could be introduced notwithstanding a phase-lock precision of 0.1  $\mu\text{sec}$  or better. The magnitude of this error has never been established theoretically for the ground wave. It is the purpose of this paper, therefore, to investigate the error quantitatively. This will be accomplished by using a suitable mathematical model for the transmitted pulse together with the mathematical definition of a particular point on the envelope of the pulse. The propagation of this point-in-time on the pulse envelope is then considered by the direct evaluation of the Fourier-transform integral appropriate to such a pulse. The theory of propagation of the continuous time-harmonic wave will be introduced as a transform of the propagation medium to take into account both the media and the effect of the boundaries.

<sup>5</sup> U. S. Naval Observatory, Contract No. (62285)9870-0373-62 with Collins Radio Co., Dallas, Tex.

## THEORY

The transient electromagnetic field  $E(t, d)$  volts per meter or  $H(t, d)$  ampere-turns per meter, at a time  $t$  and a distance  $d$  are the fundamental physical quantities described by Maxwell's equations,

$$\nabla \times \bar{E} + \mu_0 \frac{\partial}{\partial t} \bar{H} = 0$$

$$\nabla \times \bar{H} - \epsilon_0 \frac{\partial}{\partial t} \bar{E} = \bar{J},$$

where  $\bar{j}$  is a conduction or convection current, amperes per square meter and  $\mu_0$  and  $\epsilon_0$  are the permeability or permittivity of space, respectively. These equations are ordinarily solved for time-harmonic waves such that the  $(\partial/\partial t)\bar{E} = i\omega\bar{E}$ , when the frequency  $f = \omega/2\pi$ . Such a solution can be considered to be a transform in the frequency domain,  $E(\omega, d)$ ,  $H(\omega, d)$ . It is not necessary to solve Maxwell's equations again for the transient solution since this can be obtained directly from the Fourier integral utilizing the time-harmonic solution, provided a linear amplitude dependence is assumed,

$$E(t', d) = \frac{1}{2\pi} \int_{-\infty}^{\infty} \exp(i\omega t) E(\omega, d) f_r(\omega) \cdot \int_0^{\infty} \exp(-i\omega t) F_s(t) dt d\omega, \quad (1)$$

where  $F_s(t)$  specifies the form or shape of the dipole source current-moment and  $f_r(\omega)$  is the transfer function of the equipment or instrumentation. The local time  $t'$  is defined by

$$t' = t - \eta \frac{d}{c} \sim t - d/c, \quad (2)$$

where  $c$  is the speed of light in space [ $c \sim 2.997925(10^8)$  meters per second and  $\eta$  is the index of refraction of the air medium ( $\eta \sim 1.000338$ ) for air at the surface of the earth. The application of Fourier integral techniques to an electromagnetic pulse (light wave) in a region of anomalous dispersion was described many years ago by Sommerfeld<sup>6</sup> and Brillouin<sup>7</sup> in companion papers which in effect defined a signal or pulse velocity of propagation which was always less than the speed of light  $c$ , since the local time  $t'$  at which the pulse exhibited measurable amplitude was always finite,  $t' > 0$ . These arguments were followed by Johler<sup>4</sup> Wait,<sup>8,9</sup> and others in the analysis of LF signals in the time domain. Indeed, it was found to be quite possible to define a point-in-time on the leading edge of a pulse precisely. Further-

more, it is possible to study the behavior of such a point-in-time as a function of distance  $d$  and the electrical properties of the propagation media. The method known as the "amplitude envelope minus the time derivative of the amplitude envelope" method has an experimental analog<sup>3</sup> and has been described theoretically by Johler<sup>4,10</sup>. Thus, the root,  $t' = T_c$  of the equation,

$$F(t', d) = C_1 |E(t', d)| - C_2 \frac{d}{dt'} |E(t', d)| = 0, \quad (3)$$

where  $C_1$  and  $C_2$  are constants of the measuring device which set the local point-in-time on the pulse at which the measurement is to be made, describes a precise point on the pulse. The values of the constants  $C_1$  and  $C_2$  or the ratio  $C_2/C_1$  ordinarily remain constant in a measuring device as the distance  $d$  from the source of the pulse is changed.

The numerical techniques for the direct evaluation of the Fourier transform-integral have been described in detail<sup>4,11,12</sup> and various mathematical models of a general nature have been employed to describe the source current moment form or shape  $F_s(t)$ . Indeed, experimentally observed waveforms of the field can be employed in lieu of a theoretical source function.<sup>11</sup> However, for purposes of analysis of the time of propagation of a pulse, it is desirable to specify the source function  $F_s(t)$  theoretically in a manner which can be employed to synthesize or precisely specify a radio navigation pulse shape. This is accomplished<sup>4,10</sup> by superposition of three damped sinusoids as a sine-squared pulse,

$$F_s(t) = A_1 \exp(-\nu t) + A_2 \exp(-\nu_1 t) + A_3 \exp(-\nu_2 t), \quad (4)$$

where

$$\begin{aligned} \nu &= c_1 + i\omega_c, \\ \nu_1 &= c_1 + i(\omega_c + 2\omega_p), \\ \nu_2 &= c_1 + i(\omega_c - 2\omega_p), \end{aligned}$$

and

$$E(t', d) = A_1 E_{\nu}(t', d) + A_2 E_{\nu_1}(t', d) + A_3 E_{\nu_2}(t', d), \quad (5)$$

where  $A_1 = i/2$ ,  $A_2 = -i/4$ , and  $A_3 = -i/4$ . Each such damped sinusoid is characterized by the damping factor  $c_1$  the characteristic frequency,  $f_c = \omega_c/2\pi$  and the envelope frequency,  $f_p = \omega_p/2\pi$ . Since the Loran-C is a

<sup>10</sup> J. R. Johler, "A note on the propagation of certain LF pulses utilized in a radio navigation system," NBS Technical Note No. 118, PB161619, U. S. Dept. of Commerce, Office of Technical Services, Washington 25, D.C., October 27, 1961.

<sup>11</sup> J. R. Johler and C. M. Lilley, "Ground conductivity determinations at low radio frequencies by an analysis of the spheric signatures of thunderstorms," *J. Geophys. Res.*, vol. 66, pp. 3233-3244, October, 1961.

<sup>12</sup> J. R. Johler and L. C. Walters, "Propagation of a ground-wave pulse around a finitely conducting spherical earth from a damped sinusoidal source current," *IRE TRANS. ON ANTENNAS AND PROPAGATION*, vol. AP-7, pp. 1-10; January, 1959.

<sup>6</sup> A. Sommerfeld, "Über die Fortpflanzung des Lichtes in Dispergierenden Medien," *Ann. Physik.*, vol. 44, pp. 177-202; October, 1914.

<sup>7</sup> L. Brillouin, "Über die Fortpflanzung des Lichtes in Dispergierenden Medien," *Ann. Physik.*, vol. 44, pp. 203-240; October, 1914.

<sup>8</sup> J. R. Wait, "Transient fields of a vertical dipole over homogeneous curved ground," *Can. J. Phys.*, vol. 34, p. 116, January, 1956.

<sup>9</sup> J. R. Wait, "The transient behavior of the electromagnetic ground wave over a spherical earth," *IRE TRANS. ON ANTENNAS AND PROPAGATION*, vol. AP-5, pp. 198-205; April, 1957.

100-kc system,  $f_c = 100$  kc. Obviously a variety of damping factors  $c_1$  and envelope frequencies  $f_p$  can be employed to change the shape of the pulse. Since the source function  $F_s(t)$  is complex, (4), the fields  $E(t', d)$  and  $E_r(t', d)$ , (1) and (5), are complex. The amplitude envelope of the pulse  $|E(t', d)|$  has therefore been synthesized together with the pulse  $\text{Re } E(t', d)$ . This amplitude envelope can be identified with the measured envelope in the measuring device as a result of a detection process.

Each damped sinusoid can be written as follows:

$$E_r(t', d) = \frac{1}{2\pi} \int_0^\infty |E(\omega, d)| \left\{ \begin{aligned} & \left[ \frac{\cos \left[ \omega t' - \phi_c' + \tan^{-1} \frac{-(\omega_c + \omega)}{c_1} \right]}{\sqrt{c_1^2 + (\omega_c + \omega)^2}} \right. \\ & + \left. \frac{\cos \left[ -\omega t' + \phi_c' + \tan^{-1} \frac{-(\omega_c - \omega)}{c_1} \right]}{\sqrt{c_1^2 + (\omega_c - \omega)^2}} \right] \\ & + i \left[ \frac{\sin \left[ \omega t' - \phi_c' + \tan^{-1} \frac{-(\omega_c + \omega)}{c_1} \right]}{\sqrt{c_1^2 + (\omega_c + \omega)^2}} \right. \\ & + \left. \left. \frac{\sin \left[ -\omega t' + \phi_c' + \tan^{-1} \frac{-(\omega_c - \omega)}{c_1} \right]}{\sqrt{c_1^2 + (\omega_c - \omega)^2}} \right] \right\} d\omega, \quad (6) \end{aligned} \right.$$

where

$$\phi_c' = \phi_c - \frac{\pi}{2},$$

and the transform for ground-wave propagation around the surface of the terrestrial sphere a distance  $d$  is

$$E(\omega, d) \exp(i\omega t) = |E(\omega, d)| \exp \left\{ i \left[ \omega t' - \phi_c(\omega, d) + \frac{\pi}{2} \right] \right\}. \quad (7)$$

Eq. (7) can be evaluated by the series of residues,

$$E(\omega, d) = i\omega C \left[ 2\pi\alpha^{2/3}(k_1 a)^{1/3} \frac{d}{a} \right]^{1/2} \sum_{s=0}^{\infty} \frac{\exp \left\{ -i \left[ (k_1 a)^{1/3} \tau_s \alpha^{2/3} \frac{d}{a} + \frac{\alpha d}{2a} + \frac{\pi}{4} \right] \right\}}{2\tau_s - 1/\delta_e^2} \quad s = 0, 1, 2, 3 \dots, \quad (8)$$

where

$$k_1 = \frac{\omega}{c} \eta_1, \quad (9)$$

$$k_2 = \frac{\omega}{c} \left[ \epsilon_2 - i \frac{\sigma \mu_0 c^2}{\omega} \right]^{1/2}, \quad (10)$$

$$\delta_e = \frac{i(k_2^2/k_1^2)\alpha^{1/3}}{(k_1 a)^{1/3} [(k_2^2/k_1^2) - 1]^{1/2}}, \quad (11)$$

and  $\mu_0 = 4\pi(10^{-7})$  henry per meters,  $\alpha = 0.75-0.85$  and  $\tau = \tau_s$  are the special roots of Riccati's differential equation,

$$\frac{d\delta}{d\tau} - 2\delta^2\tau + 1 = 0 \quad (\delta = \delta_e), \quad (12)$$

which have been tabulated.<sup>13</sup>

$$\frac{d}{dt'} E_r(t', d) = \frac{1}{2\pi} \int_0^\infty |E(\omega, d)| \left\{ \begin{aligned} & \left[ \frac{-\omega \sin \left[ \omega t' - \phi_c' + \tan^{-1} \frac{-(\omega_c + \omega)}{c_1} \right]}{\sqrt{c_1^2 + (\omega_c + \omega)^2}} \right. \\ & + \frac{\omega \sin \left[ -\omega t' + \phi_c' + \tan^{-1} \frac{-(\omega_c - \omega)}{c_1} \right]}{\sqrt{c_1^2 + (\omega_c - \omega)^2}} \right] \\ & + i \left[ \frac{\omega \cos \left[ \omega t' - \phi_c' + \tan^{-1} \frac{-(\omega_c + \omega)}{c_1} \right]}{\sqrt{c_1^2 + (\omega_c + \omega)^2}} \right. \\ & + \left. \left. \frac{\omega \cos \left[ -\omega t' + \phi_c' + \tan^{-1} \frac{-(\omega_c - \omega)}{c_1} \right]}{\sqrt{c_1^2 + (\omega_c - \omega)^2}} \right] \right\} \quad (13) \end{aligned} \right.$$

and,

$$\begin{aligned} \frac{d}{dt'} E(t', d) &= \frac{d}{dt'} E_r(t', d) + \frac{d}{dt'} E_{v_1}(t', d) \\ &+ \frac{d}{dt'} E_{v_2}(t', d). \end{aligned} \quad (14)$$

Therefore, (3) can be written,

$$C_1 |E(t', d)| - C_2 \frac{d}{dt'} |E(t', d)| \cdot \cos \left[ \arg \frac{d}{dt'} E(t', d) - \arg E(t', d) \right]. \quad (15)$$

<sup>13</sup> J. R. Johler, L. C. Walters, and C. M. Lilley, "Low- and very low-radio-frequency tables of ground-wave parameters for the spherical earth theory: the roots of Riccati's differential equation," NBS Tech. Note No. 7, PB-151366, U. S. Dept. of Commerce, Office of Technical Services, Washington, D. C.; February, 1959.

The complex spectrum,  $F_x(\omega, d)$ , is defined,

$$F_x(\omega, d) = |f(\omega, d) + f(-\omega, d)| \cdot \exp [i \arg \{f(\omega, d) + f(-\omega, d)\}], \quad (\omega \geq 0) \quad (16)$$

where the transform is defined,

$$f(\omega, d) = E(\omega, d) \int_0^{\infty} \exp(-i\omega t) F_s(t) dt. \quad (17)$$

The quadrature techniques for evaluating the integrals, in (6), (13) and (17), have been described by Jöhler and Lilley.<sup>11</sup>

#### ANALYSIS OF THE NAVIGATION-TIMING PULSE

The synthesis of various shape sine-squared  $F_s(t)$  dipole-source current moments is illustrated in Fig. 1. The  $\text{Re } F_s(t)$  is shown. Since a complex source function  $F_s(t)$  is employed (4), the amplitude envelope (dashed line) is automatically synthesized by the values of the complex frequencies,  $\nu, \nu_1, \nu_2$ . The value of the envelope frequency  $f_p$  is varied from 1 kc to 10 kc to illustrate various leading-edge rise times on the pulse. The ringing of the pulse at later times can be reduced by increasing the damping. This, of course, also affects the rise time of the leading edge of the pulse.

The electromagnetic fields (vertical electric) in space corresponding to these elementary dipole current moments are illustrated in Fig. 2, for the ground wave. The corresponding complex spectrum of the pulse (amplitude and phase) is illustrated in Fig. 3. Such a presentation can be employed to ascertain the significant amount of radio spectrum occupied by the pulse. Thus, the width of the spectrum amplitude to the  $(2)^{-1/2}$  voltage points is indicated as varying from 12 kc to 66 kc for these pulse shapes at very short distances (1.86 statute miles). The spectrum mutilation at the greater distances by the propagation transform  $E(\omega, d)$  will attenuate the higher frequencies,<sup>4</sup> since the ground-wave transfer function appears to be a low-pass filter. It is noted in this analysis that a perfect measuring device,  $f_r(\omega) = 1$ , will be assumed, since the purpose of the analysis is to define the propagation time of the pulse. Obviously, the transfer function of the measuring device,  $f_r(\omega) \neq 1$ , is a complex number which can be introduced at this point in the analysis as part of the complex spectrum  $F_x(\omega, d)$ .

A particular dipole source current pulse together with the electromagnetic field at various distances and various ground conductivities are illustrated in Fig. 4. Note that the pulse slips in time to the right (later time) as the conductivity is decreased or the distance increased. This can be readily ascertained from Fig. 4 by noting that the pulse takes on appreciable amplitude at even later time relative to  $t' = 0$  as the conductivity is decreased or the distance increased. Also, the zero crossings of a particular cycle under the pulse can be compared to deduce this slipping in time. Indeed, the

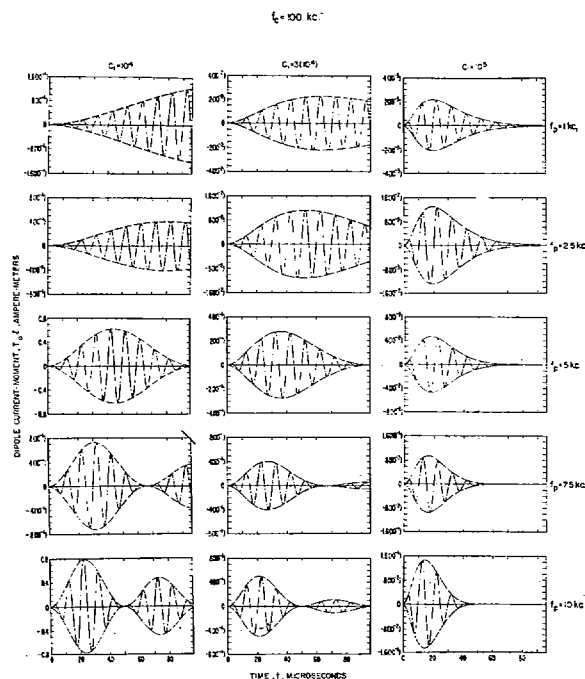


Fig. 1—Dipole source current moments as a function of time,  $I_{0l} = F_s(t)$ ,  $I_{0l} \pm 1$ , illustrating synthesis of various pulse shapes, together with the amplitude envelope (dashed curves)  $|F_s(t)|$ .

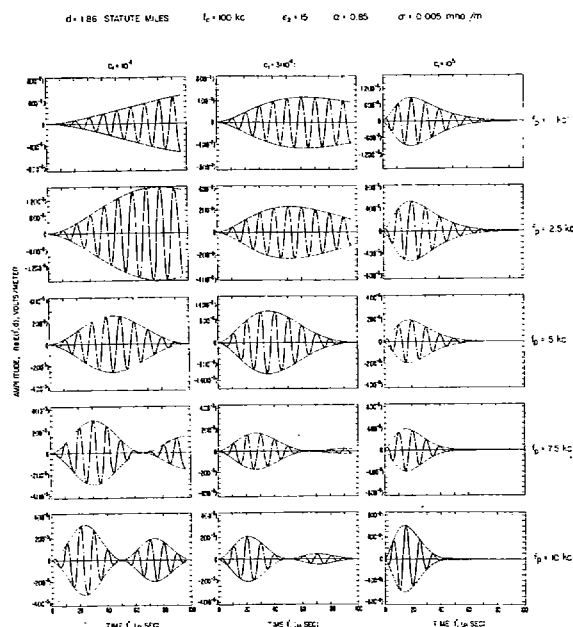


Fig. 2—Electromagnetic (vertical electric) field resulting from pulsed dipole source current moment at a short distance from the source.

pulse slips to the later time by amounts greater than  $2\pi$  radians or  $10 \mu\text{sec}$  at 100 kc. The amount of slip in time is not necessarily a linear function of distance, *i.e.*, the signal velocity has a small distance dependence.

The distortion of the individual cycles under the pulse envelope at early times ( $< 20 \mu\text{sec}$ ) on the pulse is illustrated Fig. 5. The cycle distortion becomes quite small after the second cycle has occurred at distances as great as 2000 statute miles from the source over

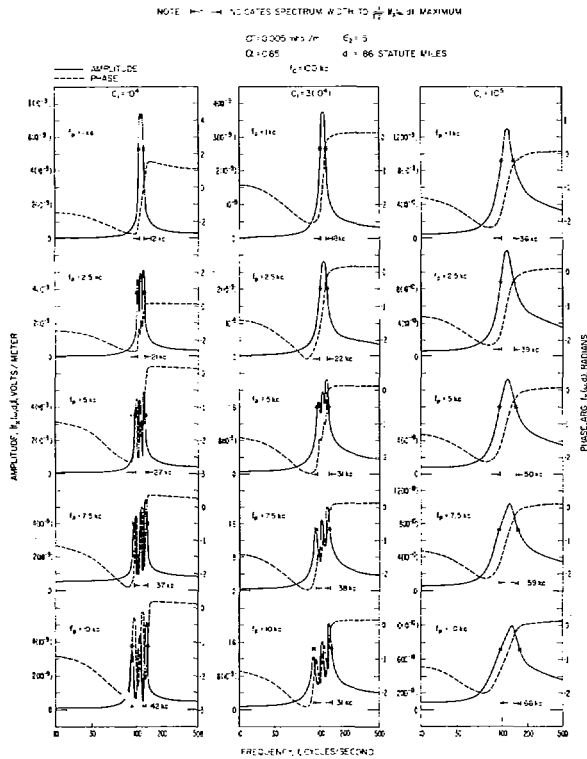


Fig. 3—Amplitude  $|F_2(\omega, d)|$  and phase  $\arg F_2(\omega, d)$  spectrum at short distance from the source for the various-shaped pulses.

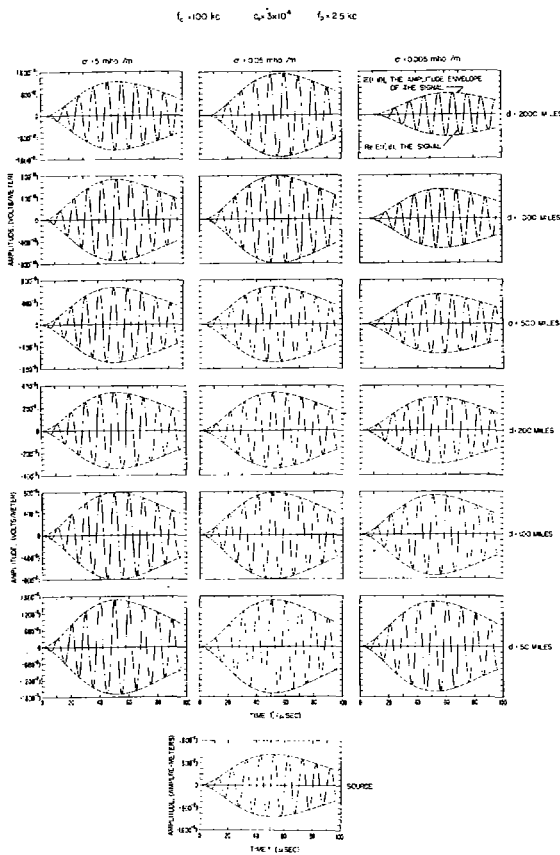


Fig. 4—Electromagnetic (vertical electric) field,  $\text{Re } E(t, d)$  resulting from a pulsed dipole source current-moment at various distances  $d$  from the source, and ground conductivity  $\sigma$  illustrating a slipping of the pulse in time as distance is increased or conductivity, decreased.

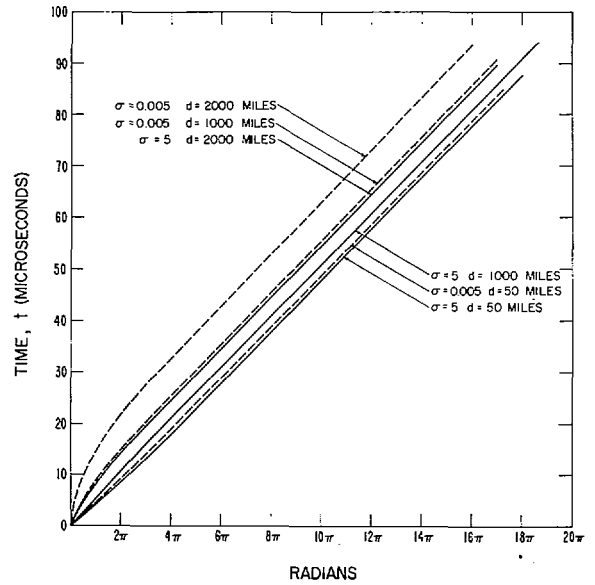


Fig. 5—Time as a function of zero crossing times of cycles under envelope of pulse illustrating phase distortion at early times ( $<20 \mu\text{s}$ ) on the pulse at various distances and ground conductivity.

ground conductivities as small as 0.005 mho per meter (over average land). This is obvious from the linear curve with a  $45^\circ$  slope representing the time of zero crossing of the cycle vs time.

The behavior of the amplitude envelope minus the derivative of the amplitude envelope function,  $F(t', d) = C_1|E(t', d)| - C_2(d/dt)|E(t', d)|$ , is illustrated at distances,  $d = 50, 1000$  statute miles in Figs. 6, 7, for a conductivity,  $\sigma = 0.005$  mho per meter (typical land), and in Figs. 8, 9,  $\sigma = 5$  mho per meter (sea water). The zero crossings of this function, *i.e.*, the roots of this differential equation,  $t' = T_c$ , describe a time on the leading edge of a pulse which is a measure of the pulse shape or dispersion. The point-in-time so determined is illustrated in Fig. 10 ( $\sigma = 0.005$ ) and Fig. 11 ( $\sigma = 5$ ), at various points on the leading edge of the pulse determined by the ratio,  $C_2/C_1$ . The bottom curve on these figures show the phase correction,  $t_c = \phi_c/\omega(10^6) \mu\text{sec}$  of the continuous-wave solution calculated directly from the series of residues of (8). The continuous-wave solution so determined cannot resolve a cycle ambiguity of  $\pm 2\pi n$  where  $n$  is an integer ( $n = 0, 1, 2, 3 \dots$ ) or  $\pm 10 n \mu\text{sec}$  for 100 kc. Only the transient solution together with a method for tagging a point-in-time can resolve such an ambiguity. This was realized in the design of the Loran-C system,<sup>8</sup> and the two types of detection (amplitude envelope and phase detection) were employed. The amplitude envelope detection simulated the mathematical process described in this paper by forming the root of the differential equation (3) to identify the particular cycle. The phase detector then made the precision phase measurement on the cycle thus identified. The recently developed method<sup>5</sup> for use with clock synchronization performs these two operations together, but the net result is the same. Greater instrumental precision is obtainable, however. The times

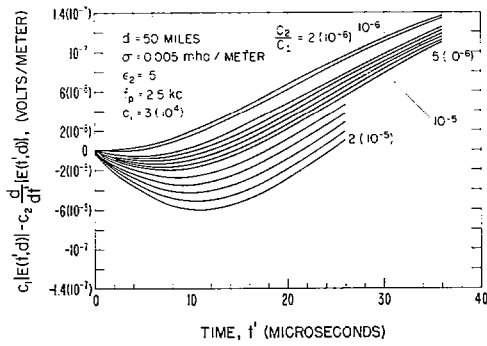


Fig. 6—The amplitude envelope minus the derivative of the amplitude envelope illustrating zero crossing on roots of  $F(t', d)$  at particular times  $t' = T_c$  for various values of  $C_2/C_1$ .

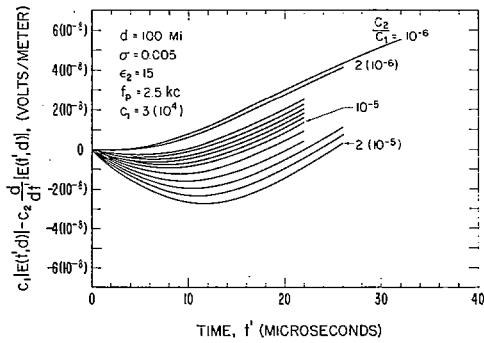


Fig. 7—The amplitude envelope minus the derivative of the amplitude envelope illustrating zero crossing of roots of  $F(t', d)$  at particular times  $t' = T_c$  for various values of  $C_2/C_1$ .

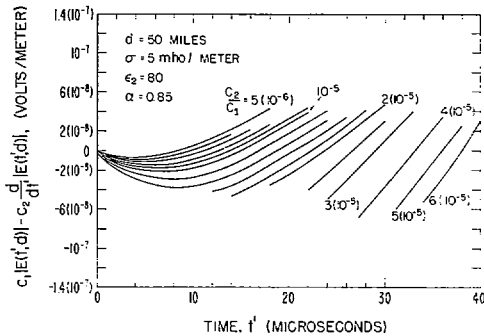


Fig. 8—The amplitude envelope minus the derivative of the amplitude envelope illustrating zero crossing of roots of  $F(t', d)$  at particular times  $t' = T_c$  for various values of  $C_2/C_1$ .

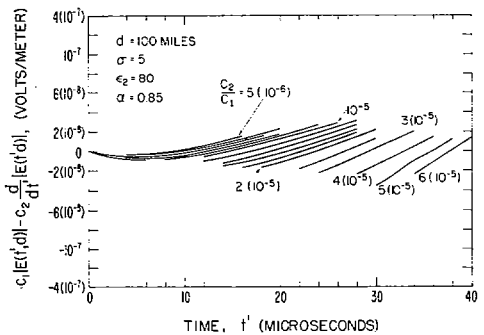


Fig. 9—The amplitude envelope minus the derivative of the amplitude envelope illustrating zero crossing of roots of  $F(t', d)$  at particular times  $t' = T_c$  for various values of  $C_2/C_1$ .

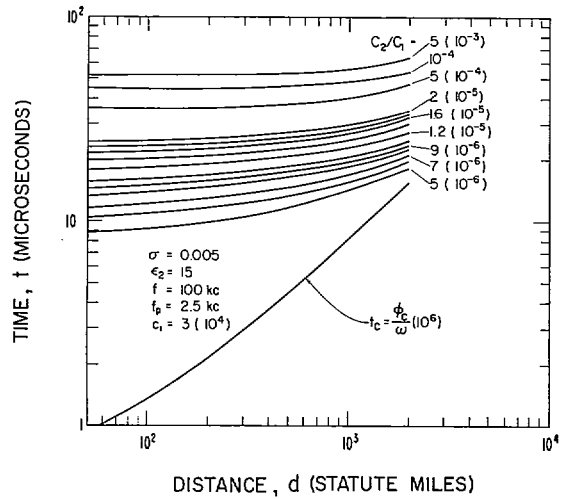


Fig. 10—Local time  $t' = T_c$  of occurrence of the tagged point on the pulse as a function of distance.

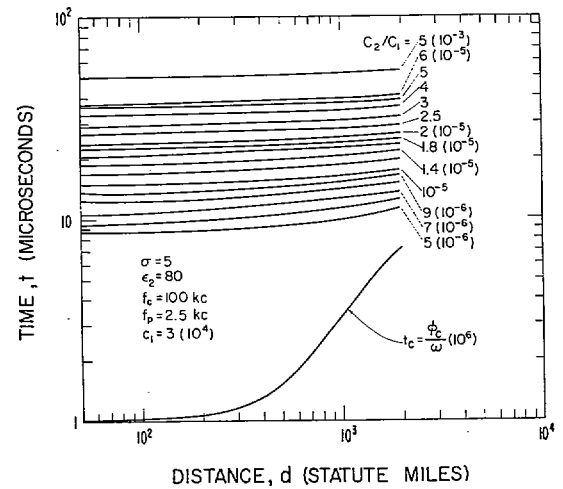


Fig. 11—Local time  $t' = T_c$  of occurrence of the tagged point on the pulse as a function of distance.

of zero crossing are illustrated in Fig. 5. Note the curvature at very early times on the pulse. Thus, the precision measurement should be made sufficiently high on the pulse so that the curvature shown in Fig. 5 at early times  $t'$  is negligible. Under such conditions the continuous-wave phase correction describes the correct propagation time. The difference between the phase measurement and the envelope measurement is obviously a criterion of the pulse dispersion. Thus, the pulse dispersion error has been established for the ground wave by determining the position of the point-in-time on the envelope of a pulse propagated over the smooth, homogeneous terrestrial sphere. The results of such a determination are illustrated Fig. 12 ( $\sigma = 0.005$ ), and Fig. 13 ( $\sigma = 5$ ). The results are also illustrated in Table I ( $\sigma = 0.005$ ) and Table II ( $\sigma = 5$ ). The random variation in the last significant figure of these tables represents the computation precision of the quadrature polynomials employed in the computation.<sup>11,12</sup> The tabulated values were normalized to  $d = 50$  statute miles from the source. Thus, it is assumed that a point is tagged at

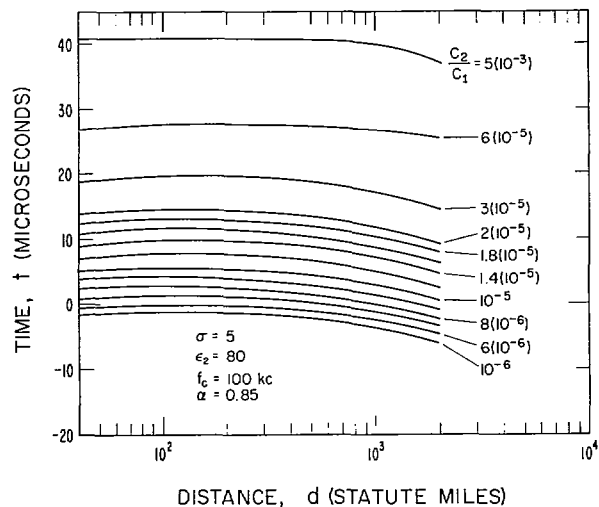
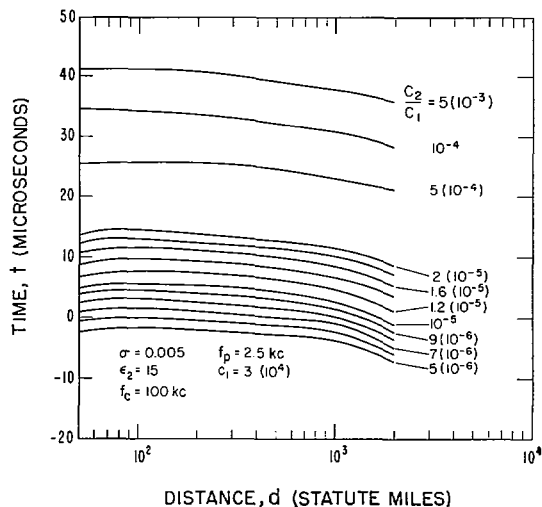


Fig. 12—The discrepancy between the continuous-wave time and the tagged-point time, illustrating pulse dispersion.

Fig. 13—The discrepancy between the continuous-wave time and the tagged-point time, illustrating pulse dispersion.

TABLE I  
SIGNAL PROPAGATION TIME OVER LAND

$\sigma = 0.005$ $\epsilon_2 = 15$		(MICROSECONDS)						$f_c = 100 \text{ kc}$ $\alpha = 0.85$
$C_2/C_1$	Fiducial Point at 50 Miles	Tagged Point-In-Time on the Pulse						
		50 Miles	100 Miles	200 Miles	500 Miles	1000 Miles	2000 Miles	
$5(10^{-6})$	9.3	0.0	0.6	0.9	3.6	5.4	9.3	
$6(10^{-6})$	10.6	0.0	0.5	1.3	3.0	6.0	9.3	
$7(10^{-6})$	11.9	0.0	0.5	1.2	2.9	5.5	8.9	
$8(10^{-6})$	13.4	0.0	0.5	1.0	2.7	5.2	8.7	
$9(10^{-6})$	14.6	0.0	0.4	1.1	2.7	5.3	8.8	
$10^{-5}$	15.8	0.0	0.4	1.1	2.7	5.2	9.0	
$1.2(10^{-5})$	17.2	0.0	0.4	1.1	2.8	5.3	9.3	
$1.4(10^{-5})$	19.8	0.0	0.4	1.1	2.8	5.4	9.6	
$1.6(10^{-5})$	21.6	0.0	0.4	1.1	2.8	5.4	9.9	
$1.8(10^{-5})$	23.2	0.0	0.4	1.1	2.8	5.3	9.9	
$2(10^{-5})$	24.6	0.0	0.4	1.1	2.8	5.3	9.9	
$3(10^{-5})$	30.1	0.0	0.4	1.1	2.8	5.4	9.8	
$4(10^{-5})$	33.9	0.0	0.4	1.1	2.8	5.4	10.6	
$5(10^{-5})$	36.6	0.0	0.4	1.1	2.7	5.1	11.7	
Continuous wave	0.851	0.0	0.534	1.325	3.583	7.930	14.87	

TABLE II  
SIGNAL PROPAGATION TIME OVER SEA WATER

$\sigma = 5$ MICROSECONDS		Tagged Point-In-Time on the Pulse					
$C_2/C_1$	Fiducial Point at 50 Miles	50 Miles	100 Miles	200 Miles	500 Miles	1000 Miles	2000 Miles
		$5(10^{-6})$	8.5	0.0	0.02	0.1	0.8
$7(10^{-6})$	11.1	0.0	0.07	0.3	0.8	1.6	2.5
$10^{-5}$	15.1	0.0	0.04	0.1	0.5	1.2	2.4
$1.2(10^{-5})$	17.0	0.0	0.04	0.3	0.9	1.6	2.8
$1.4(10^{-5})$	18.7	0.0	0.04	0.6	1.0	1.8	3.0
$1.6(10^{-5})$	20.8	9.0	0.04	0.1	0.7	1.4	2.7
$1.8(10^{-5})$	22.3	0.0	0.06	0.2	0.7	1.4	2.7
$2(10^{-5})$	23.8	0.0	0.06	0.2	0.7	1.3	2.5
$3(10^{-5})$	29.0	0.0	0.2	0.5	1.0	1.7	2.9
Continuous wave	0.0944	0.0	0.103	0.375	1.411	3.288	7.056

50 statute miles from the source, by setting  $C_2/C_1$ , a constant, into the system of measurement. Then, on increasing the distance successively to 100, 200, 500, 1000, and 2000 statute miles the discrepancy increases to values greater than  $\pi$  radians or 5  $\mu\text{sec}$ . Thus, over land the possibility of an ambiguity exists. However, with the aid of the time-correction values for the envelope, this ambiguity can be resolved. Indeed, a maximum correction of 11.7  $\mu\text{sec}$  is noted for the cases calculated. It is further noted that the possibility of an ambiguity over sea water ( $\sigma=5$ ) is less. However, the pulse dispersion or discrepancy is not negligible.

It is quite evident that Loran-C could synchronize a clock on the wrong cycle if the results (Tables I and II) were unknown irrespective of the nominal 0.1- $\mu\text{sec}$  phase-lock precision. The correct clock setting could be readily ascertained by the calculations which are demonstrated in Tables I, and II, noting that  $10 \mu\text{sec} = 2\pi$  radians or 1 cycle at 100 kc.

### CONCLUSIONS

The propagation time of a radio signal propagated via the ground wave has been determined by tagging a

point-in-time on the leading edge of a pulse. It has been found that under certain circumstances the error in the precision phase measure can be  $\pm\pi$  radians or  $\pm 5 \mu\text{sec}$  at 100 kc. The computations in this paper give the magnitude of the error, and hence allow corrections to be made in the clock synchronization system employing Loran-C. Thus, the full precision of a nominal 0.1  $\mu\text{sec}$  or better can be realized for the ground wave.

The signal time correction,  $t' = T_e$ , can be determined with the aid of the full transient solution employing a direct evaluation of the Fourier-transform integral, by specifying a pulse form or shape. Thus, the point-in-time on the pulse envelope can be evaluated, tabulated and graphed for practical use in radio navigation systems.

The results of this paper suggest an extension of the work to determine the pulse dispersion introduced by waves reflected from the ionosphere.

### ACKNOWLEDGMENT

This work was performed in consultation with Dr. W. Markowitz, Director, Time Service Division, U. S. Naval Observatory.

## Signals, Scatterers, and Statistics\*

VICTOR TWERSKY†, FELLOW, IEEE

**Summary**—In the first part of this paper we consider an ensemble of complex numbers (a set of signals in time, the field scattered by different configurations of scatterers, etc.) and obtain relations among various average functions that may be defined for such an ensemble. In particular, we consider the average total intensity, the coherent intensity, and the incoherent intensity (absolute squared functions of the ensemble); the coherent phase, average phase and average-square phase; the variances of the real and imaginary components of the ensemble and their covariance (or equivalently, the second moments of any phase-quadrature components of the field), as well as the higher moments. The second moments are represented in terms of the incoherent intensity and the real and imaginary parts of an "asymmetry function"  $P$ ; if  $P=0$ , then the variances are equal and the covariance is zero. In the second part of the paper, we briefly sketch the formalism that leads to scattering function representations for the intensities and coherent phase, and then develop the corresponding scattering representation of the new function  $P$ . We illustrate the development by explicit results for "gas-like" random distributions of large tenuous scatterers. Thus we obtain direct relations between the various statistical functions mentioned above and

the fundamental parameters of the scattering problem. Since the parameters enter differently in the various averages, and since these functions can be measured simultaneously and independently, the results facilitate inverting measured data.

### I. INTRODUCTION

IN STATISTICAL scattering and propagation studies, based either on an ensemble of spatial configurations of scatterers ("scatterer statistics"),<sup>1,2</sup> or on an ensemble of time-varying signals ("signal statistics"),<sup>3,4</sup> we may deal with various average functions of a complex valued field. We may consider absolute squared functions of the field, *i.e.*, the average intensity,

<sup>1</sup> V. Twersky, "On scattering of waves by random distributions," I, Free-space scatterer formalism," *J. Math. Phys.*, vol. 3, pp. 700-715, 1962; II, "Two-space scatterer formalism," vol. 3, pp. 724-234; 1962.

<sup>2</sup> V. Twersky, "On scattering by quasi-periodic and quasi-random distributions," *IRE TRANS. ON ANTENNAS AND PROPAGATION*, vol. AP-7, pp. 5307-5319; December, 1959.

<sup>3</sup> S. O. Rice, "Statistical properties of a sine wave plus random noise," *Bell Sys. Tech. J.* vol. 10, pp.109-157; 1948 (plus many other papers).

<sup>4</sup> H. Bremmer, "Propagation of electromagnetic waves," in "Handbuch der Phys." Springer, Berlin, Germany, vol. 16, p. 432; 1958.

\* Received August 10, 1962; revised manuscript received April 24, 1963. This work was partially supported by U. S. Signal Corps Contracts.

† Sylvania Electronic Defence Laboratories, Mountain View, California; now also at the Mathematics Dept., Technion—Israel Institute of Technology, Haifa.